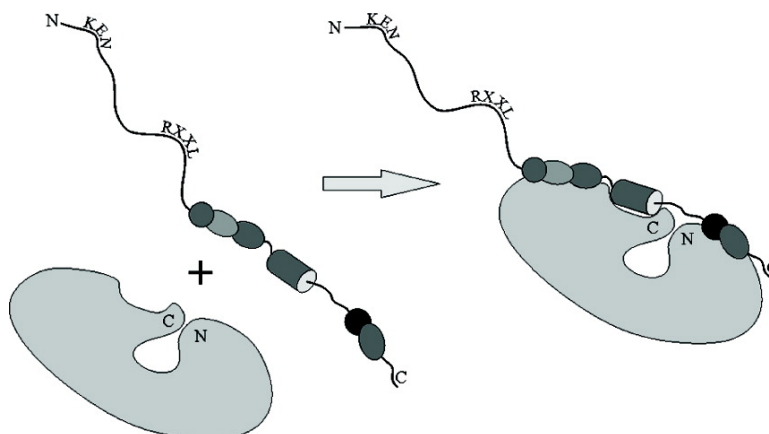


Structural and Dynamic Characterization of Intrinsically Disordered Human Securin by NMR Spectroscopy

Veronika Csizmok, Isabella C. Felli, Peter Tompa, Lucia Banci, and Ivano Bertini

J. Am. Chem. Soc., **2008**, 130 (50), 16873-16879 • DOI: 10.1021/ja805510b • Publication Date (Web): 18 November 2008

Downloaded from <http://pubs.acs.org> on February 8, 2009



More About This Article

Additional resources and features associated with this article are available within the HTML version:

- Supporting Information
- Access to high resolution figures
- Links to articles and content related to this article
- Copyright permission to reproduce figures and/or text from this article

[View the Full Text HTML](#)

Structural and Dynamic Characterization of Intrinsically Disordered Human Securin by NMR Spectroscopy

Veronika Csizmok,[†] Isabella C. Felli,[‡] Peter Tompa,^{*,†} Lucia Banci,[‡] and Ivano Bertini[‡]

Institute of Enzymology, Biological Research Center, Hungarian Academy of Sciences, Budapest, Karolina ut 29, H-1113, Hungary, and Center of Magnetic Resonance (CERM), Department of Chemistry, University of Florence, Via Sacconi 6, 50019 Sesto Fiorentino, Italy

Received February 21, 2008; E-mail: tompa@enzim.hu

Abstract: Understanding the molecular action of securin, the inhibitor of separase in mitosis, is of immense theoretical and biomedical importance. The residue-level structural description of an intrinsically disordered protein of this length (202 amino acids, containing 24 prolines), however, represents a particular challenge. Here we combined ¹H-detected and ¹³C-detected *protonless* NMR experiments to achieve full assignment of securin's backbone amide resonances. Chemical shifts, ¹⁵N relaxation rates (R_1 , R_2 , ¹H–¹⁵N NOEs), ¹H exchange rates with the solvent (CLEANEX-PM), and ¹H–¹⁵N residual dipolar couplings were determined along the entire length of the protein. This analysis showed that securin is not entirely disordered, but segregates into a largely disordered N-terminal half and a C-terminal half with transient segmental order, within which the segment D¹⁵⁰-F¹⁵⁹ has a significant helical tendency and segments E¹¹³-S¹²⁷ and W¹⁷⁴-L¹⁷⁸ also show a significant deviation from random-coil behavior. These results, in combination with bioinformatic and biochemical data on the securin/separase interaction, shed light on the inhibitory action of securin on separase.

Introduction

The proper execution of mitosis in a cell division cycle requires precise regulation of separase, the protease responsible for the physical separation of sister chromatids, by its inhibitor, securin.^{1–3} Separase cleavage of the Scc1/Mcd1/Rad21 cohesin subunit, which holds sister chromatids together, in the metaphase–anaphase transition is critical for the maintenance of euploidy. Securin, which holds separase in an inactive state until the onset of anaphase, is polyubiquitinated at both its destruction box (RxxL) and KEN box motifs and is rapidly degraded in the metaphase–anaphase transition. Securin also acts as a chaperone of separase activity, targeting the latter to the nucleus,^{2,4} and has additional functions, primarily related to DNA repair and apoptosis.^{5,6} Due to its critical roles in controlling cell division, securin is a proto-oncogene product in humans (also called pituitary tumor transforming gene 1 product, PTTG1); i.e., its mutations cause neoplastic transformations in cancers.²

Despite its having such crucial functions, evolutionary relations in the separase/securin system are rather enigmatic.

Separases in various species are generally large proteins with a molecular mass around 200 kDa, of which only the proteolytic C-terminal part shows discernible sequence conservation.^{7,8} Securins, functionally identified in *Saccharomyces cerevisiae* (Pds1p⁹), *Schizosaccharomyces pombe* (Cut2¹⁰), *Drosophila melanogaster* (pimples¹¹), and *Homo sapiens* (PTTG1), on the other hand, are extremely variable in length and show practically no recognizable similarity in sequence, except for short segments in the N-terminus. Possible structural–functional similarity is also present in their C-terminal 100 amino acids, which are responsible for separase inhibition^{4,7,12} and probably lack a well-defined structural state.^{13,14}

Numerous proteins or protein domains, termed intrinsically disordered proteins (IDPs) or intrinsically unstructured proteins (IUPs), lack a well-defined 3D structure, yet they carry out important functions in the cell in signal transduction and transcription regulation.^{15–17} Disorder provides various functional advantages, such as binding plasticity and high specificity but low affinity, and thus it is rather common in different

[†] Hungarian Academy of Sciences.

[‡] Center of Magnetic Resonance (CERM).

- (1) Zou, H.; McGarry, T. J.; Bernal, T.; Kirschner, M. W. *Science* **1999**, *285*, 418–422.
- (2) Jallepalli, P. V.; Waizenegger, I. C.; Bunz, F.; Langer, S.; Speicher, M. R.; Peters, J. M.; Kinzler, K. W.; Vogelstein, B.; Lengauer, C. *Cell* **2001**, *105*, 445–457.
- (3) Waizenegger, I.; Gimenez-Abian, J. F.; Wernic, D.; Peters, J. M. *Curr. Biol.* **2002**, *12*, 1368–1378.
- (4) Hornig, N. C.; Knowles, P. P.; McDonald, N. Q.; Uhlmann, F. *Curr. Biol.* **2002**, *12*, 973–982.
- (5) Hamid, T.; Kakar, S. S. *Mol. Cancer* **2004**, *3*, 18.
- (6) Nagao, K.; Adachi, Y.; Yanagida, M. *Nature* **2004**, *430*, 1044–1048.

- (7) Jager, H.; Herzig, B.; Herzig, A.; Sticht, H.; Lehner, C. F.; Heidmann, S. *Cell Cycle* **2004**, *3*, 182–188.
- (8) Viadiu, H.; Stemmann, O.; Kirschner, M. W.; Walz, T. *Nat. Struct. Mol. Biol.* **2005**, *12*, 552–553.
- (9) Yamamoto, A.; Guacci, V.; Koshland, D. J. *Cell. Biol.* **1996**, *133*, 85–97.
- (10) Hirano, T.; Funahashi, S. I.; Uemura, T.; Yanagida, M. *EMBO J.* **1986**, *5*, 2973–2979.
- (11) Leismann, O.; Herzig, A.; Heidmann, S.; Lehner, C. F. *Genes Dev.* **2000**, *14*, 2192–2205.
- (12) Nagao, K.; Yanagida, M. *Genes Cells* **2006**, *11*, 247–260.
- (13) Cox, C. J.; Dutta, K.; Petri, E. T.; Hwang, W. C.; Lin, Y.; Pascal, S. M.; Basavappa, R. *FEBS Lett.* **2002**, *527*, 303–308.
- (14) Sanchez-Puig, N.; Veprintsev, D. B.; Fersht, A. R. *Protein Sci.* **2005**, *14*, 1410–1418.

proteomes.^{18–20} Detailed structural characterization of securin would not only extend our knowledge of IDPs but also be critical for understanding securin–separase interaction in molecular detail, with the prospect of developing effective small-molecule antagonists of securin.

The detailed structural characterization of an IDP, however, represents a particular challenge because these proteins exist as an ensemble of rapidly interconverting conformations with functionally important, but transient, long- and short-range structural organization.^{21–23} The residue-level description of the conformational distribution and its correlation with function can only be achieved by multidimensional NMR.^{24,25} Several interesting examples have recently appeared.^{26–33} Such an analysis, however, is hampered by reduced chemical shift dispersion caused by the lack of a structure, which precludes the study of larger IDPs. In this context, human securin with its 202 amino acids, including 24 prolines, represents a challenge that requires the combination of traditional proton-based and newly devised *protonless* NMR techniques.^{34–36} Protonless NMR experiments,^{26,34} in particular those based on carbonyl direct detection,^{26,35} are very well suited to study IDPs thanks to their relatively high residual carbonyl chemical shift dispersion and the ability to detect proline residues, often abundant in IDPs. By this novel approach, we show that securin is mostly disordered, but it contains some transient local structural elements, marked by chemical shift values, ¹⁵N relaxation rates (R_1 , R_2 , ¹H–¹⁵N NOEs), ¹H exchange rates with the solvent (CLEANEX-PM), ¹H–¹⁵N residual dipolar couplings deviating

from those of purely random coil conformations. Correlation of these observations with previous biochemical data and with sequence comparisons suggests that these regions may critically contribute to securin function. Direct experimental evidence that one of these regions is important for the interaction with separase is provided here. The progress in the understanding of the structural details of the securin/separase interaction will provide critical information toward developing specific securin antagonists.

Experimental Section

Preparation of Human Securin. The full-length cDNA of human securin was amplified by polymerase chain reaction from the pRSETHisLipoTev plasmid kindly provided by Prof. Sir Alan Fersht (Gonville and Caius College, Cambridge University, UK), and ligated into a pET20b plasmid (Novagen), which contains a 6-residue-long His-tag fused to the C-terminal end of the insert (pET20b-human securin). The plasmid pET20b-human securin was transformed into *Escherichia coli* strain BL21 Star. Cultures were grown in minimal medium supplemented with ¹³C-glucose and/or (¹⁵NH₄)₂SO₄ and 100 μg/mL ampicillin to an optical density of 0.8 at 600 nm, induced with 0.5 mM isopropyl 1-thio-β-D-galactopyranoside (IPTG), and incubated overnight at 30 °C. The protein was purified from the pellet obtained after sonication (7 × 10 s, 24 mμ) and centrifugation (20 min, 20000g). The pellet was dissolved in a buffer of 50 mM Tris, 300 mM NaCl, pH 7.5, containing 6 M urea and further incubated for 3 h. After incubation, the solution was centrifuged at 100000g for 30 min at 4 °C, and the supernatant was loaded on a NiNTA column (Qiagen). The protein was dialyzed into 25 mM Na₂HPO₄, 150 mM KCl, and 10 mM 2-mercaptoethanol, pH 7.2, and the final concentration of NMR samples was 0.7 mM. To exclude the effect of aggregation, one experiment (CBCACON) was repeated, on a protein sample diluted 4 times (0.175 mM final protein concentration); 10% D₂O was added for the lock signal.

Preparation of the Catalytic Domain of Human Separase.

cDNA of the full-length human separase was kindly provided by Marc W. Kirschner (Harvard Medical School, Boston, MA). Human separase consists of an unstructured central stretch that separates an N-terminal half of armadillo (ARM) repeats from the two C-terminal caspase domains, i.e., the catalytic domain of the protein.⁸ Upon securin degradation, the active site becomes accessible, which leads to an autocleavage of the protein at EILR¹⁵⁰⁶ or ELLR¹⁵³⁵, releasing its catalytic domain.³ cDNA of the catalytic domain (E¹⁵⁰³–R²¹²⁰) was amplified by high-fidelity DNA polymerase and subcloned into the *NdeI*–*XhoI* sites of the expression vector pET20b (Novagen). The construct was verified by DNA sequencing (MWG-Biotech).

The catalytic domain of separase was expressed in the *E. coli* strain BL21 Star. Expression was induced by 0.5 mM IPTG at 30 °C for 3 h. The protein was purified from the pellet obtained after sonication (7 × 10 s, 24 mμ) and centrifugation (20 min, 20000g). The pellet was dissolved in a buffer of 50 mM Tris, 300 mM NaCl, pH 7.5, containing 8 M urea and further incubated for 3 h. After incubation, the solution was centrifuged at 100000g for 30 min at 4 °C, and the supernatant was loaded on a NiNTA column (Qiagen). The protein was dialyzed into 50 mM Tris, 150 mM NaCl, and 1 mM EDTA, pH 7.5, and the final concentration was 1.5 μM. The proper fold of the protein was verified by CD measurements (data not shown).

CD Experiments. CD experiments were carried out on ¹⁵N human securin (about 6 μM concentration) in 25 mM Na₂HPO₄ buffer, pH 7.4, and on the synthesized peptide comprising residues 150–159 (about 50 μM) in water on a JASCO J-810 spectropolarimeter. The CD spectrum obtained after baseline subtraction is reported in the Supporting Information (Figure S1A,B).

NMR Experiments and Data Analysis. The ¹H-detected and ¹³C-detected *protonless* NMR experiments for sequence-specific resonance assignment and for the determination of residual dipolar

- (15) Tompa, P. *FEBS Lett.* **2005**, *579*, 3346–3354.
- (16) Uversky, V. N.; Oldfield, C. J.; Dunker, A. K. *J. Mol. Recognit.* **2005**, *18*, 343–384.
- (17) Dyson, H. J.; Wright, P. E. *Nat. Rev. Mol. Cell Biol.* **2005**, *6*, 197–208.
- (18) Dunker, A. K.; Obradovic, Z.; Romero, P.; Garner, E. C.; Brown, C. J. *Genome Inform. Ser. Workshop Genome Inform.* **2000**, *11*, 161–171.
- (19) Ward, J. J.; Sodhi, J. S.; McGuffin, L. J.; Buxton, B. F.; Jones, D. T. *J. Mol. Biol.* **2004**, *337*, 635–645.
- (20) Tompa, P.; Dosztanyi, Z.; Simon, I. *J. Proteome Res.* **2006**, *5*, 1996–2000.
- (21) Dobson, C. M. *Nature* **2003**, *426*, 884–890.
- (22) Smith, L. J.; Fiebig, K. M.; Schwalbe, H.; Dobson, C. M. *Fold Des.* **1996**, *1*, R95–106.
- (23) Daggett, V.; Fersht, A. R. *Trends Biochem. Sci.* **2003**, *28*, 18–25.
- (24) Dyson, H. J.; Wright, P. E. *Chem. Rev.* **2004**, *104*, 3607–3622.
- (25) Mittag, T.; Forman-Kay, J. D. *Curr. Opin. Struct. Biol.* **2007**, *17*, 3–14.
- (26) Bermeil, W.; Bertini, I.; Felli, I. C.; Lee, Y. M.; Luchinat, C.; Pierattelli, R. *J. Am. Chem. Soc.* **2006**, *128*, 3918–3919.
- (27) Sivakolundu, S. G.; Bashford, D.; Kriwacki, R. W. *J. Mol. Biol.* **2005**, *353*, 1118–1128.
- (28) Rasia, R. M.; Bertocini, C. W.; Marsh, D.; Hoyer, W.; Cherny, D.; Zweckstetter, M.; Griesinger, C.; Jovin, T. M.; Fernandez, C. O. *Proc. Natl. Acad. Sci. U.S.A.* **2005**, *102*, 4294–4299.
- (29) Vise, P. D.; Baral, B.; Latos, A. J.; Daughdrill, G. W. *Nucleic Acids Res.* **2005**, *33*, 2061–2077.
- (30) Mukrasch, M. D.; von Bergen, M.; Biernat, J.; Fischer, D.; Griesinger, C.; Mandelkow, E.; Zweckstetter, M. *J. Biol. Chem.* **2007**, *282*, 12230–12239.
- (31) Eliezer, D.; Barre, P.; Kobaslija, M.; Chan, D.; Li, X.; Heend, L. *Biochemistry* **2005**, *44*, 1026–1036.
- (32) Sillen, A.; Barbier, P.; Landrieu, I.; Lefebvre, S.; Wieruszkeski, J. M.; Leroy, A.; Peyrot, V.; Lippens, G. *Biochemistry* **2007**, *46*, 3055–3064.
- (33) Landrieu, I.; Lacosse, L.; Leroy, A.; Wieruszkeski, J. M.; Trivelli, X.; Sillen, A.; Sibille, N.; Schwalbe, H.; Saxena, K.; Langer, T.; Lippens, G. *J. Am. Chem. Soc.* **2006**, *128*, 3575–3583.
- (34) Bermeil, W.; Bertini, I.; Felli, I. C.; Piccioli, M.; Pierattelli, R. *Prog. NMR Spectrosc.* **2006**, *48*, 25–45.
- (35) Bermeil, W.; Bertini, I.; Felli, I. C.; Kummerle, R.; Pierattelli, R. *J. Magn. Reson.* **2006**, *178*, 56–64.
- (36) Bertini, I.; Duma, L.; Felli, I. C.; Fey, M.; Luchinat, C.; Pierattelli, R.; Vasos, P. R. *Angew. Chem., Int. Ed.* **2004**, *43*, 2257–2259.

couplings were carried out at 283 K on a 16.4 T Bruker AVANCE 700 spectrometer, operating at 700.13 MHz for ^1H and 176.08 MHz for ^{13}C , equipped with a new-generation cryogenically cooled probe optimized for ^{13}C sensitivity as well as for ^1H sensitivity.

A data set consisting of a combination of ^{13}C -detected *protonless* (CON-IPAP, CBCACON-IPAP, and CBCANCO-IPAP) and ^1H -detected (HSQC, HNC0, CBCACONH, CBCANH, and HN(CA)N-NH) NMR experiments was necessary for sequence-specific assignment of H^{N} , N , C' , C^{α} , and C^{β} resonances. ^1H - ^{15}N residual dipolar couplings were acquired with the IPAP approach. Experimental details are reported in the Supporting Information (Table S1).

To further characterize the structural and dynamic features of human securin, the following ^1H -detected NMR experiments were also acquired (at 283 K on a 11.7 T Bruker AVANCE 500 spectrometer equipped with a cryoprobe): ^{15}N relaxation experiments (R_1 , R_2 , with different τ_{CPMG} values and ^1H - ^{15}N NOEs) and CLEANEX-PM experiments. Experimental details are reported in the Supporting Information (Table S1).

One-bond ^1H - ^{15}N residual dipolar couplings were measured on human securin aligned in 5% (w/v) *n*-octyl-penta(ethylene glycol)/octanol (C_8E_5 , Sigma).³⁷ Residual dipolar couplings were determined by taking the difference between the ^1H - ^{15}N splittings (in absolute value) measured for human securin with and without addition of an "orienting" medium (deuterium splitting observed 27.5 Hz).

Data were processed with Topspin and were analyzed with the program CARA.³⁸ The secondary structure propensity from the chemical shifts was determined by the approach described in ref 39, with random-coil reference chemical shift values,⁴⁰ corrected for primary sequence as described in ref 41.

Far Western Blot and *in Vitro* Protein–Peptide Binding Assay. The far Western blot analysis was performed according to Wu et al.⁴² Human securin and the catalytic domain of human separase were dialyzed into 50 mM Tris buffer (pH 7.5) containing 50 mM NaCl and 1 mM EDTA. Human securin and bovine serum albumin (BSA, control) were separated by SDS–PAGE, transferred to a nitrocellulose membrane, incubated with the catalytic domain of separase (0.074 μM) for 2 h, washed with PBS, and visualized by anti-separase antibody kindly provided by Dr. Stefan Heidmann (Department of Genetics, University of Bayreuth, Bayreuth, Germany).

The *in vitro* protein–peptide binding assay was performed in the same buffer as indicated above. The catalytic domain of human separase was separated by SDS–PAGE, transferred to a nitrocellulose membrane, denatured/renatured with sequential guanidin $\cdot\text{HCl}$ dilution (from 6 M to 0 M) on the membrane, and incubated with biotinylated securin peptide (biotinyl-NH-GGGDEERELEKLFGGG-COOH) obtained from Bio-Science Trading Ltd. After a short washing step with PBS, it was further incubated with streptavidin–alkaline phosphatase and visualized with BCIP/NBT reagent (Sigma).

Results

NMR Sequence-Specific Assignment of Human Securin. The construction and expression protocol for human securin was improved compared to the protocol used by Sanchez-Puig et al.¹⁴ to allow the preparation of isotopically labeled samples (^{15}N and $^{15}\text{N}/^{13}\text{C}$) in the millimolar concentration range, suitable for ^{13}C NMR detection. Previous NMR data suggested an overall

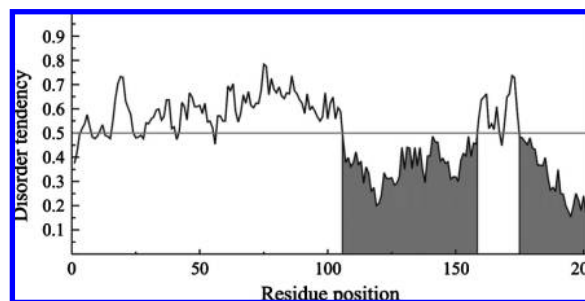


Figure 1. Prediction of structural disorder of securin. Disorder propensity was predicted by the IUPred algorithm.^{51,52} Score values above the threshold of 0.5 are considered disordered (white), whereas score values below 0.5 are considered ordered (gray).

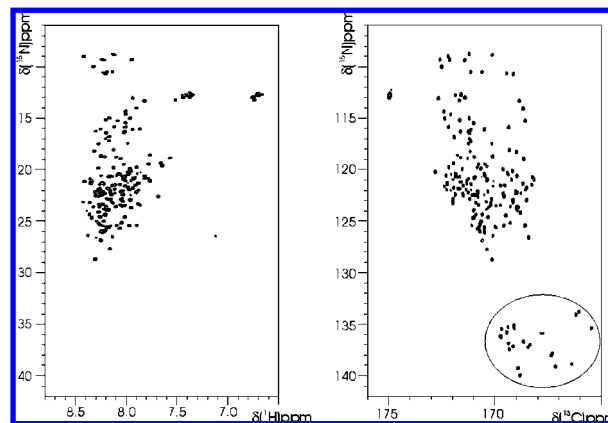


Figure 2. Comparison of ^1H - ^{15}N HSQC (left) and ^{13}C - ^{15}N CON-IPAP (right) spectra. The ^1H - ^{15}N HSQC and ^{13}C - ^{15}N CON-IPAP spectra of human securin are shown to illustrate the additional information content from *protonless* NMR experiments. In the ^{13}C - ^{15}N CON-IPAP spectrum, the circle indicates the proline residues.

disorder of human securin.¹⁴ Prediction through the use of bioinformatic tools (see below), however, shows that the C-terminal half has some tendency to be ordered (Figure 1), whereas the N-terminal half is entirely disordered. To achieve a residue-resolution picture of the structural and dynamic behavior of the protein, we had to achieve full assignment of H^{N} , N , C' , C^{α} , and C^{β} resonances.

To this end, a set of data comprising ^1H -detected and ^{13}C -detected *protonless* NMR experiments was analyzed. The additional information content coming from *protonless* NMR experiments based on carbonyl direct detection^{26,34,35} can be appreciated by comparing ^1H - ^{15}N HSQC and ^{13}C - ^{15}N CON-IPAP 2D experiments (Figure 2). A first count in the two spectra indicates 122 well-resolved backbone cross peaks in the HSQC, which corresponds to 60% of the residues (68% of the expected correlations; i.e., all amino acids excluding Pro-s and the first residue), and 165 in the CON-IPAP, which corresponds to 82% of the residues, which essentially coincides with the expected correlations. This increase in number is due to the intrinsically higher resolution of the CON-IPAP experiment. Moreover, the high number of prolines, quite common in IDPs, contributes an additional 22 cross peaks at the characteristic shift of N of proline residues in the CON-IPAP 2D map (Figure 2), while they are obviously not observed in HSQC experiments. Therefore, the *protonless* NMR experiments, based on C' direct detection and on ^{15}N resonances in the indirect dimension, significantly increase the information content of the ensemble of the experiments for sequence-specific assignment.

- (37) Otting, G.; Ruckert, M. *J. Am. Chem. Soc.* **2000**, *122*, 7793–7797.
 (38) Keller, R. L. J. *The Computer Aided Resonance Assignment Tutorial (1.3)*; CANTINA Verlag: 2004.
 (39) Berjanskii, M.; Wishart, D. S. *Nat. Protoc.* **2006**, *1*, 683–688.
 (40) Wishart, D. S.; Bigam, C. G.; Holm, A.; Hodges, R. S.; Sykes, B. D. *J. Biomol. NMR* **1995**, *5*, 67–81.
 (41) Schwarzingler, S.; Kroon, G. J.; Foss, T. R.; Chung, J.; Wright, P. E.; Dyson, H. J. *J. Am. Chem. Soc.* **2001**, *123*, 2970–2978.
 (42) Wu, Y.; Li, Q.; Chen, X. Z. *Nat. Protoc.* **2007**, *2*, 3278–3284.

In the CBCACON-IPAP³⁵ experiment, 193 sets of cross peaks ($C'_i, C^{\alpha}_i, N_{i+1}$, $C'_i, C^{\beta}_i, N_{i+1}$) out of the 201 expected could be readily identified by the typical patterns of correlations expected, including 22 sets of cross peaks involving proline nitrogens, characterized by a specific ¹⁵N chemical shift, while in the analogous proton-detected 3D experiment (CBCACONH), 171 sets of cross peaks ($C'_i, C^{\alpha}_i, H^N_{i+1}$, $C'_i, C^{\beta}_i, H^N_{i+1}$) are detected.

The combination of ¹H-detected and ¹³C-detected *protonless* NMR experiments enabled us to obtain a nearly complete sequence-specific assignment of H^N, N, C', C^α, and C^β resonances (97% C', 99% C^α and C^β, 97% H^N, and 98% N). The chemical shifts are reported in the Supporting Information (Table S2). The present approach therefore provides a valuable tool for complete sequence-specific assignment of unfolded systems, including a new strategy to overcome the problem of prolines interrupting the “sequence-specific walk”, compared to the previously proposed ones based on ¹H detection.^{43,44} Our strategy is particularly suitable for unfolded proteins, where the ¹H chemical shift dispersion is limited. As an example, a few strips taken from the ¹H-detected and ¹³C-detected *protonless* NMR experiments (segment SVPA¹⁰⁶) are given in the Supporting Information (Figures S2 and S3).

Structural Features of Human Securin. Chemical shifts are very sensitive to the local environment, represented by both sequentially and spatially neighboring amino acids.^{45,46} Obviously, the contribution of the latter is largely reduced if the protein has no stable 3D structure.^{47,48} The difference between the experimentally measured and the random-coil chemical shifts,⁴⁰ properly corrected for the primary sequence,⁴⁹ can indicate whether a given protein segment attains, for some fraction of time, some secondary structure. The actual data, shown in Figure 3, are consistent with an α -helical secondary structure propensity⁵⁰ for the region D¹⁵⁰-F¹⁵⁹. Indeed, in this region both C^α (Figure 3A), C^α-C^β (Figure 3B), and C' (Figure 3C) shifts are positive, and further confirmation comes from the ¹⁵N shifts (Figure 3D). The magnitude of the observed shifts indicates that about 30% of the conformers in the ensemble adopt an α -helical conformation. In other regions, non-zero residual shift values also indicate localized conformations, although they do not point to any specific secondary structural element. The helical propensity of a protein segment is in agreement with CD measurements, which show a small amount (less than 10%) of α -helical secondary structure (Supporting Information, Figure S1A) in the full-length protein. Moreover, a high tendency to adopt an α -helical secondary structure is found for the peptide including D¹⁵⁰-F¹⁵⁹ from both CD and NMR evidence (Supporting Information, Figure S1B,C). Analy-

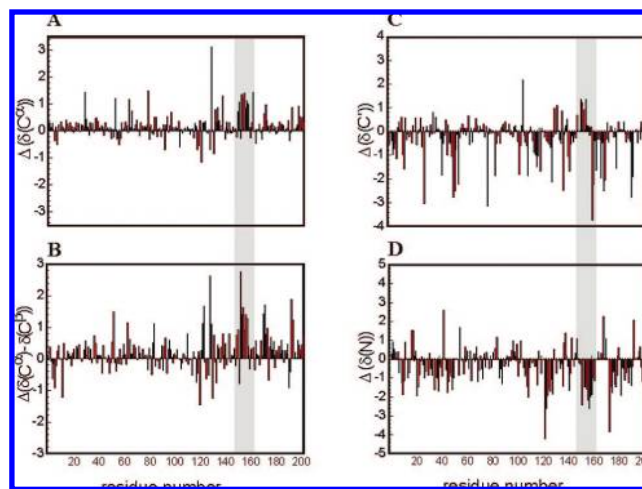


Figure 3. Assessment of secondary structural preferences in securin. Differences (in ppm) of the observed chemical shifts with respect to reference values characteristic of the random-coil conformation of small peptides,⁶⁶ properly corrected to account for the contributions by sequential neighbors,⁴¹ are shown: (A) C^α carbons, (B) C^α-C^β carbons, (C) C' carbons, and (D) N amide nitrogens. Gray shading marks the region D¹⁵⁰-F¹⁵⁹ with significant local helical propensity (for explanation, see text).

ses with IUPred^{51,52} and other bioinformatic tools, such as PONDR and DisPred, to predict the degree of local order for intrinsically disordered sequences are in agreement with a local decrease of disorder in this region. Predictors of secondary structure, such as the Gor IV algorithm,⁵³ indicate an α -helical structure for this segment.

To confirm these findings and to obtain additional clues for the remaining part of the protein, other NMR observables were measured. These measures, such as ¹⁵N relaxation rates (R_1 , R_2 , ¹H-¹⁵N NOEs), ¹H exchange rates with the solvent (CLEANEX-PM), and ¹H-¹⁵N residual dipolar couplings (RDCs), are useful probes of the behavior of amino acids in intrinsically disordered systems and can highlight the relative propensity of different fragments of the primary sequence for local, fractional conformations. The analysis of these data is reported in Figure 4. In folded proteins, heteronuclear NOEs, which are very sensitive to local motions faster than the overall tumbling of the molecule, are usually positive and close to 1, while for random-coil polypeptide chains they are negative. In human securin, NOEs show several changes in sign along the amino acid chain (Figure 4A), with regions characterized by fast motions and high flexibility (negative NOEs) and regions characterized by slower motions. The latter behavior can suggest a tendency to adopt transiently folded conformations. Regions characterized by more than four residues in a row with positive NOEs are 113–134 and 149–159 (cf. gray shading in Figure 4). Other residues characterized by positive values are 10, 11, 15, 16, 20, 24, 139, 167, 174, 175, 177, and 178, which essentially highlight two other regions with reduced motions on the nanosecond time scale, namely 10–24 and 174–178. These results confirm the structural preferences of the region 149–159, and highlight other regions, in particular 10–24, 113–134, and 174–178, with reduced motions on the nanosecond time scale. Interestingly, these regions mainly cluster in the C-terminal part of the protein, in agreement with the disorder score calculated by IUPred (Figure 1).

- (43) Bottomley, M. J.; Macias, M. J.; Liu, Z.; Sattler, M. *J. Biomol. NMR* **1999**, *13*, 381–385.
 (44) Kanelis, V.; Donaldson, L.; Muhandiram, D. R.; Rotin, D.; Forman-Kay, J. D.; Kay, L. E. *J. Biomol. NMR* **2000**, *16*, 253–259.
 (45) Case, D. A.; Dyson, H. J.; Wright, P. E. *Methods Enzymol.* **1994**, *239*, 392–416.
 (46) Wishart, D. S.; Case, D. A. *Methods Enzymol.* **2001**, *338*, 3–34.
 (47) Yao, J.; Dyson, H. J.; Wright, P. E. *FEBS Lett.* **1997**, *419*, 285–289.
 (48) Schwalbe, H.; Fiebig, K. M.; Buck, M.; Jones, J. A.; Grimshaw, S. B.; Spencer, A.; Glaser, S. J.; Smith, L. J.; Dobson, C. M. *Biochemistry* **1997**, *36*, 8977–8991.
 (49) Schwarzinger, S.; Kroon, G. J. A.; Foss, T. R.; Wright, P. E.; Dyson, H. J. *J. Biomol. NMR* **2000**, *18*, 43–48.
 (50) Marsh, J. A.; Singh, V. K.; Jia, Z.; Forman-Kay, J. D. *Protein Sci.* **2006**, *15*, 2795–2804.
 (51) Dosztanyi, Z.; Csizmok, V.; Tompa, P.; Simon, I. *Bioinformatics* **2005**, *21*, 3433–3434.
 (52) Dosztanyi, Z.; Csizmok, V.; Tompa, P.; Simon, I. *J. Mol. Biol.* **2005**, *347*, 827–839.

- (53) Garnier, J.; Gibrat, J. F.; Robson, B. *Methods Enzymol.* **1996**, *266*, 540–553.

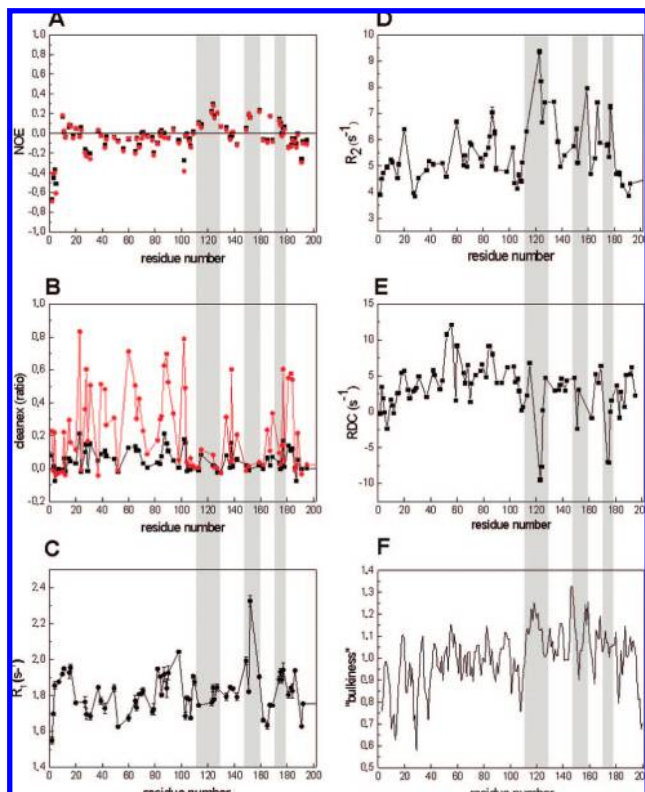


Figure 4. ^{15}N relaxation parameters (R_1 , R_2 , ^1H – ^{15}N NOEs), HN exchange effects, and ^1H – ^{15}N RDCs for amide groups of human securin. (A) ^1H – ^{15}N NOEs (the two values are derived from independent experiments to give an estimate of the precision of the measurement). (B) Ratio of CLEANEX cross peaks (black, 5 ms; red, 10 ms). (C) ^{15}N R_1 . (D) ^{15}N R_2 . (E) ^1H – ^{15}N RDCs measured in an alignment medium. (F) The “bulkiness” function as defined by Zweckstetter and Blackledge,⁵⁵ multiplied by the bell-shaped function.⁴⁸ Gray shading marks regions with significant local structural features (for explanation, see text).

The CLEANEX-PM experiments (Figure 4B) provide information on exchange processes of amide protons with the solvent, which are characteristic of solvent exposure. The first half of the protein is characterized by efficient exchange processes with the solvent, as measured by the increase of cross peaks with the increase in the CLEANEX “mixing time”. In particular, regions 15, 23, 27–31, 39–49, and 60–103 show high cross peak intensities, indicating efficient exchange with the solvent, i.e., little protection. The latter behavior is also observed for residues 177 and 181–184. In contrast, regions 113–134 and 149–159 do not show appreciable cross peaks due to solvent exchange at either of the mixing times, indicating a relatively more protected, i.e., structured, local environment within the C-terminal part. Again, some scattered residues are also identified that do not give rise to exchange, indicating some protection also in the first part of the primary sequence (residues 3, 5, 7, 10, 12, 16, 20, 24, 37, and 52).

Analysis of ^{15}N relaxation rates (R_1 and R_2), and particularly of R_2 , shows a bell-like profile characterized by a central plateau and lower rates at the edges, as expected for unfolded systems (Figure 4C,D), according to the simple segmental motion model.⁴⁸ Some stretches have R_2 values much higher than the plateau, in particular residues 113–134, 149–159, and 167–177, and some scattered residues at positions 20, 60, 85–89, and 103 (Figure 4D). R_2 values higher than the plateau can be due either to a more structured conformation or to exchange processes, or to both effects occurring simultaneously, which

can be the case in unfolded proteins. Therefore, R_2 values higher than the plateau are generally interpreted as originating from a stretch of a protein which deviates from the simple segmental motion model.⁴⁸ Overall, this behavior of human securin points to a significant deviation from random-coil behavior for the region 149–159, where an α -helical secondary structure propensity was observed, as well as for the regions 113–134 and 167–177 and for some scattered residues in the initial part of the protein, one of them in the 10–24 region.

Residual dipolar coupling values are also sensitive indicators of local order and report on both structural and dynamic features of the protein. Conformational averaging between various conformers in unfolded proteins is expected to reduce the magnitude of RDCs, and indeed the observed values for human securin average to about +3 Hz (Figure 4E). Interestingly, they do not average to zero, indicating that the protein does not sample an isotropic distribution of conformations, as expected for a random polypeptide chain.⁵⁴ Moreover, in addition to a bell-like distribution expected for *random flight chains*,⁵⁴ a high variability is observed throughout the polypeptide chain. A correlation between the magnitude of RDC and the bulkiness of the amino acid side chains has been recently observed.⁵⁵ It is worth noting that the regions mentioned above, i.e., 113–134 and 167–177, are characterized by a higher content of hydrophobic or bulky residues (Figure 4F and Supporting Information, Figure S5). However, for several residues the RDC values cannot be accounted for by the “bulkiness criteria”, as they display much higher positive RDCs, with the highest values for residues 52, 56, 60, 84, and 85–87, or negative RDCs (below -1 Hz) for residues 7, 123–124, 151, and 174–175. Interestingly, the segment 149–159 is characterized by RDCs with alternating signs and values quite close to the average but contains one of the few residues characterized by a negative RDC, indicative of a higher propensity for local order. For the other stretches, extreme values are observed within the C-terminal half and in particular within two of the regions already noted for increased local order, namely 123–124 and 174–175. The relatively larger values observed in the first part of the sequence (52, 56, 60, 84, and 85–87) seem to highlight some germs of local order, already indicated by the higher R_2 values, also in this part of the protein.

Interaction of Securin with Separase. In order to understand better the securin–separase interaction, the results of the NMR characterization of human securin were used as input for further bioinformatic and biochemical analysis of the interaction. The most unambiguous structural information on human securin from all NMR experiments is the α -helical content in the region D¹⁵⁰–F¹⁵⁹. This could be an important element of partner recognition, in agreement with the general notion that short, transiently structured segments in IDPs correspond to elements of binding to the partner, in the present case inhibition of separase by securin. Since the mode of interaction with the inhibitor is expected to share some similarities with that of interaction with the natural substrate, it was interesting to identify if any segment with sequence similarity to the D¹⁵⁰–F¹⁵⁹ of human securin is present in the Scc1 cohesin subunit, the real substrate of separase. The alignment of human securin and the Scc1 subunit of human cohesin shows that the D¹⁵⁰–F¹⁵⁹ region of the securin aligns best with the separase cleavage site in the Scc1 (Sup-

(54) Louhiouri, M.; Paakkonen, K.; Fredriksson, K.; Permi, P.; Lounila, J.; Annala, A. *J. Am. Chem. Soc.* **2003**, *125*, 15647–15650.

(55) Cho, M. K.; Kim, H. Y.; Bernado, P.; Fernandez, C. O.; Blackledge, M.; Zweckstetter, M. *J. Am. Chem. Soc.* **2007**, *129*, 3032–3033.

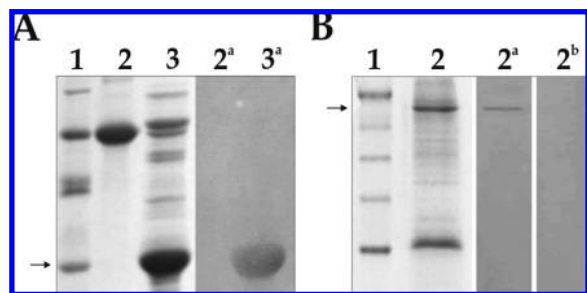


Figure 5. Interaction of human separase with securin. (A) Far Western blot analysis of the interaction between the recombinant catalytic domain of human separase and the full-length human securin. Protein marker (lane 1), bovine serum albumin (BSA) as control protein (lane 2), and full-length human securin (lane 3) were visualized by Coomassie staining after SDS-PAGE. BSA (lane 2^a) and human securin (lane 3^a) were separated by SDS-PAGE, transferred to nitrocellulose, overlaid with separase catalytic domain, and visualized by anti-separase antibody. The arrow shows full-length human securin. (B) *In vitro* protein-peptide binding assay of the interaction between the catalytic domain of human separase and a synthetic biotinylated peptide corresponding to the D¹⁵⁰-F¹⁵⁹ region of human securin. Protein marker (lane 1) and purified catalytic domain of human separase (lane 2) were visualized by Coomassie staining after SDS-PAGE. The catalytic domain of human separase was transferred to nitrocellulose, incubated with (lane 2^a) or without (lane 2^b) the peptide, overlaid with streptavidin-alkaline phosphatase, and visualized by BCIP/NBT reagent. The arrow shows the catalytic domain of the human separase.

porting Information, Figure S6A). We interpreted the structural preference and this sequence similarity with the substrate of the separase to imply that this region is the potential site for separase recognition. To inspect this proposed interaction between separase and the D¹⁵⁰-F¹⁵⁹ region of securin, we cloned and expressed the C-terminal catalytic domain of human separase (E¹⁵⁰³-R²¹²⁰). Far Western blot analysis (Figure 5A) showed interaction between separase and the full-length securin. The interaction was then checked between the separase and the peptide corresponding to the D¹⁵⁰-F¹⁵⁹ region of securin. The securin peptide also contains a biotin on the N-terminus, which allows its detection via an interaction with streptavidin-alkaline phosphatase. An interaction could be detected between separase and the securin peptide, which was suggested to be the likely site of interaction by the above NMR, prediction, and sequence similarity studies (Figure 5B). These observations indicate that recombinant separase and securin interact specifically through the D¹⁵⁰-F¹⁵⁹ segment of securin.

Discussion

The enhanced flexibility, conformational heterogeneity, and rapid interconversion between different conformations characteristic of IDPs have recently been proposed to confer functional advantages.^{15–17} Within regions of disorder, however, segments characterized by different motional properties or by transient sampling of local order and/or secondary structural elements may represent the seeds for recognition of partner and the subsequent acquisition of folded conformations.^{56–58} In this context, NMR provides a unique, atomic-level description of motions at different time scales, of exchange processes, and of propensity to adopt a more ordered local conformation. The

intrinsic high flexibility and the low fraction of sampled folded conformations, however, greatly reduce the chemical shift dispersion. Therefore, sequence-specific assignment becomes increasingly complex with increases in the length of the polypeptide chain. The use of recently developed ¹³C-detected *protonless* NMR experiments,^{26,34,36,59,60} in combination with the ¹H-detected ones, was key to perform the full sequence-specific assignment of human securin, including prolines, which are located in stretches characterized by high flexibility and local disorder and are often implicated in protein-protein interactions.^{57,61,62} The subsequent analysis of different NMR observables, sensitive to structural, dynamic, and exchange properties in different ways, allowed us to have a complete description of the different behavior of regions in the polypeptide chain.

The most unequivocal structural information on the conformational ensemble of securin is the α -helical propensity of the region D¹⁵⁰-F¹⁵⁹, which falls within the region thought to interact with separase in other securins^{4,7,12} (Supporting Information, Figure S7). It was shown that the C-terminus of securin from *Ss. pombe* (Cut2) physically interacts with separase, and its central 76-amino-acid fragment blocks sister chromatid separation by inhibiting the enzyme.¹² In securin from *D. melanogaster* (pimples) a central segment inhibits separase,⁷ whereas in *S. cerevisiae* securin (Pds1p) inhibitory potential residues in the C-terminal 100 residues.⁴ Furthermore, the D¹⁵⁰-F¹⁵⁹ region of human securin aligns best with part of the sequences in the Scc1 subunit of human cohesin (Supporting Information, Figure S6A), which is the protein recognized and cleaved by separase. This sequence correlation provides further evidence that this region is the site of separase recognition, as experimentally verified through direct interaction assays (Figure 5B), and suggests a possible structural basis for the mechanism through which securin inhibits separase. This inference is in line with the general notion that short, transiently structured segments in IDPs correspond to elements of partner recognition. These regions are termed preformed structural elements,⁵⁶ linear motifs,⁵⁷ or molecular recognition features (MoRFs).⁵⁸ Although these are defined in somewhat different ways, the D¹⁵⁰-F¹⁵⁹ region identified in human securin appears to satisfy the criteria for being such a recognition element. In human securin the region D¹⁵⁰-F¹⁵⁹ is mainly acidic, with its N-terminal stretch DEE¹⁵³ actually being very similar to the DIE motif of securin from *Ss. pombe* (Cut2), which was shown to be responsible for the inhibition of separase (Cut1).

Other regions, such as E¹¹³-S¹²⁷ and W¹⁷⁴-Leu¹⁷⁸, sample transient local order. Intriguingly, all these regions fall into the C-terminal half of the molecule, which is predicted by IUPred and other bioinformatic tools, such as PONDR and DisPred, to tend to be more ordered than the first half, and which harbors the inhibitory activity of securins.^{4,7,12}

The N-terminal part of human securin contains both the destruction box (RxxL) and the KEN box, which mediate the degradation of the protein at the onset of anaphase. IUPred, other predictions, and NMR data suggest that the N-terminal half of securin is largely disordered and has very limited residual structure. If the C-terminal half binds separase, the protruding

(56) Fuxreiter, M.; Simon, I.; Friedrich, P.; Tompa, P. *J. Mol. Biol.* **2004**, *338*, 1015–1026.

(57) Fuxreiter, M.; Tompa, P.; Simon, I. *Bioinformatics* **2007**, *23*, 950–956.

(58) Mohan, A.; Oldfield, C. J.; Radivojac, P.; Vacic, V.; Cortese, M. S.; Dunker, A. K.; Uversky, V. N. *J. Mol. Biol.* **2006**, *362*, 1043–1059.

(59) Bermeil, W.; Bertini, I.; Duma, L.; Felli, I. C.; Emsley, L.; Pierattelli, R.; Vasos, P. R. *Angew. Chem., Int. Ed.* **2005**, *44*, 3089–3092.

(60) Bermeil, W.; Bertini, I.; Felli, I. C.; Kümmerle, R.; Pierattelli, R. *J. Am. Chem. Soc.* **2003**, *125*, 16423–16429.

(61) Williamson, M. P. *Biochem. J.* **1994**, *297*, 249–260.

(62) Kay, B. K.; Williamson, M. P.; Sudol, M. *Faseb. J.* **2000**, *14*, 231–241.

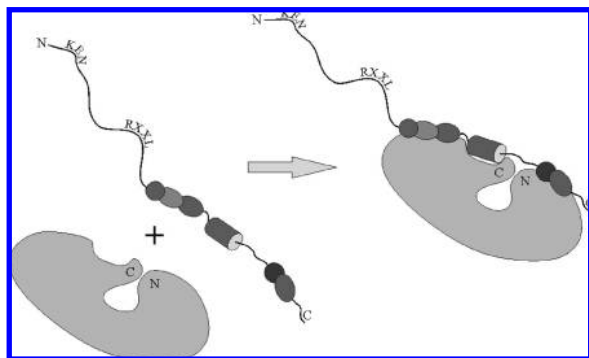


Figure 6. Putative model of the securin–separase interaction. The key features are as follow: (i) the protruding N-terminal disordered region serves for ubiquitination and degradation, (ii) the middle segment including the helical D¹⁵⁰–F¹⁵⁹ region inhibits the C-terminal (catalytic) region of separase, and (iii) the C-terminal region binds the N-terminal half of the enzyme, preventing the large-scale conformational change required for its activation. This model is consistent with our data on the solution state of securin, and also with prior data on the mode of securin–separase interaction.¹²

disordered N-terminal segment would be easily accessible for ubiquitination, as suggested to be a general feature in other post-translational modifications.^{57,63} This mode of recognition may ensure that even separase-bound securin might be tagged for degradation and may be accessible for recognition by other potential binding partners, such as KU, the regulatory subunit of the DNA-dependent protein kinase,⁶⁴ and PBF, the PTTG-binding factor⁶⁵ (Supporting Information, Figure S7B). A putative model of the interaction is presented in Figure 6, with the following key features: (i) the protruding N-terminal disordered region serves for ubiquitination and degradation; (ii) the middle segment, including the helical D¹⁵⁰–F¹⁵⁹ region, inhibits the C-terminal (catalytic) region of separase; and (iii) the C-terminal region binds the N-terminal half of the separase, preventing the large-scale conformational change required for its activation. This model is consistent with our structural data on the solution state of securin, and also with prior data on the mode of securin–separase interaction.¹²

The present results, together with sequence comparisons and functional/binding studies, also shed some light on the enigmatic evolution of securins. Despite their crucial role in regulating cell cycle, functionally analogous securins share practically no recognizable sequence similarity (Supporting Information, Fig-

ure S6). This apparently contradicts the classical view that functionality confers evolutionary constraints, which manifests itself as conservation of sequence. Some sort of conservation can, however, also be recognized in securin, more in its conformational properties than in its sequence patterns. These details can be interpreted in terms of a model that describes securin as a beads-on-a-string protein, with very short, somewhat conserved recognition elements embedded in a long and very variable disordered scaffold. Thus, the extreme variability of the sequence is allowed by this unusual mode of recognition and the co-evolution that also involves unusual variability of separases.

Overall, the combination of ¹H-detected and ¹³C-detected protonless NMR techniques allowed a detailed conformational and dynamical characterization of an IDP as large as human securin. Because this approach has the power of characterizing regions containing large numbers of prolines, a characteristic feature of most IDPs, it has the potential for studying even larger proteins within this structural class in the future. The various NMR observables indicated several regions, mainly clustered in the C terminal part of the protein, characterized by higher order. These findings, combined with bioinformatic tools, allowed us to make a hypothesis on one key segment of the securin involved in the interaction with separase. This hypothesis was then confirmed through biochemical assays, providing important hints on one of the key regions of the securin–separase interaction and suggesting a way securin has evolved to specifically bind its partner molecule, separase. The present work thus lays the foundation for a detailed molecular characterization of the securin–separase interaction, which will be instrumental in future efforts aimed at developing effective antagonists of securin.

Acknowledgment. This research was supported by grants K60694 and NK71582 from the Hungarian Scientific Research Fund (OTKA) and 245/2006 from the Hungarian Ministry of Health, and by the International Senior Research Fellowship, ISRF 067595, from the Wellcome Trust. All NMR experiments were acquired thanks to the EUNMR access project (contract no. RII3-026145, EU-NMR). V.C. acknowledges the support of the Marie Curie Training Site (contract no. MEST-CT-2004-504391). We are indebted to Prof. Sir Alan Fersht for the expression construct of human securin, Dr. Stefan Heidmann for the anti-separase antibody, and Dr. Marc W. Kirschner for the cDNA of the full-length human separase. Dr. Stefania Girotto (CERM, Florence, Italy) is gratefully acknowledged for acquisition and analysis of CD experiments. The MIUR-FIRB (RBLA032ZM7) project “Piattaforma NMR per lo studio dell’interazione proteine-leganti di interesse farmacologico” is gratefully acknowledged.

Supporting Information Available: Figures S1–7 and Tables S1 and S2. This material is available free of charge via the Internet at <http://pubs.acs.org>.

JA805510B

- (63) Iakoucheva, L. M.; Radivojac, P.; Brown, C. J.; O’Connor, T. R.; Sikes, J. G.; Obradovic, Z.; Dunker, A. K. *Nucleic Acids Res.* **2004**, *32*, 1037–1049.
- (64) Romero, F.; Multon, M. C.; Ramos-Morales, F.; Dominguez, A.; Bernal, J. A.; Pintor-Toro, J. A.; Tortolero, M. *Nucleic Acids Res.* **2001**, *29*, 1300–1307.
- (65) Tfelt-Hansen, J.; Yano, S.; Bandyopadhyay, S.; Carroll, R.; Brown, E. M.; Chattopadhyay, N. *Endocrinology* **2004**, *145*, 4222–4231.
- (66) Wishart, D. S.; Bigam, C. G.; Yao, J.; Abildgaard, F.; Dyson, H. J.; Oldfield, E.; Markley, J. L.; Sykes, B. D. *J. Biomol. NMR* **1995**, *6*, 135–140.